Light-induced phase transition in AlD_3 at high pressure

Stanislav P. Besedin*
Institute of Crystallography Russian Academy of Sciences, Leninskii Prospekt 59, 119333 Moscow, Russia, and Russian Research Center "Kurchatov Institute," Kurchatov Square 1, 123182 Moscow, Russia

Andrew P. Jephcoat
Diamond Light Source, Harwell Science and Innovation Campus Didcot, Oxfordshire OX11 0DE, United Kingdom, and Department of Earth Sciences, University of Oxford, Parks Road, Oxford OX1 3PR, United Kingdom

Alla V. Irodova
Russian Research Center "Kurchatov Institute," Kurchatov Square 1, 123182 Moscow, Russia
(Received 18 April 2011; revised manuscript received 27 July 2011; published 8 September 2011)

Trivalent aluminum hydride in the rhombohedral α phase ($R\bar{3}c$ space group) was studied at high pressures in a diamond-anvil cell by means of Raman scattering, x-ray diffraction, observation of optical transmission, and the density functional simulations. At $P \approx 53$ GPa the heavier isotope AlD_3 undergoes a first-order structural phase transition which was found to be stimulated by the laser irradiation used for the Raman-scattering measurements. In the new high-pressure phase Al atoms form a lattice with a monoclinic unit cell ($P2_1/c$ space group) over which a superstructure is developed when pressure is varied. The superstructure is formed by regular displacements of the Al atoms with the period over three unit cells; the propagation vector is $\mathbf{k}_2 = (\frac{1}{3}\frac{1}{3}\frac{1}{3})$. The undistorted $P2_1/c$ lattice itself appears as superstructure over the rhombohedral $R\bar{3}c$ one resulting from the displacive structure transformation with the propagation vector $\mathbf{k}_1 = (\frac{1}{2}0\frac{1}{2})$. The band gap as given by the density functional calculations and evidenced from the sample transparency behavior at high pressures remains greater than the laser photon energy used ($E_{ph} = 2.41$ eV). That indicates that bond weakening/breaking due to electron excitation across the band gap is not the cause of the phase transition. A likely mechanism of the light action is that structure transformation is driven by phonons, which are excited due to strong electron-phonon coupling in the α phase.

DOI: 10.1103/PhysRevB.84.104111 PACS number(s): 81.40.Vw, 61.50.Ks, 64.70.K−, 74.10.+v

I. INTRODUCTION

During the past years considerable attention has been paid to studies of trivalent aluminum hydride AlH_3.[1–6] Part of the interest arises from the expectation that hydrogen-rich materials can be used as hydrogen-storage systems.[5–7] Another part is connected to superconductivity in covalent-bonded materials. Strong electron-phonon coupling featuring covalent bonds and high-phonon frequencies resulting from the presence of light atoms gives rise to fairly high critical superconducting temperatures T_c (for example in MgB_2 $T_c = 40$ K).[8] The next natural question is whether higher values of T_c can be achieved.

The lightest material with covalent bonds is molecular hydrogen. In fact, metallic hydrogen has long been suggested to be a high-temperature superconductor in both the atomic[9] and the molecularlike[10] forms. Moreover, metallic hydrogen is predicted to adopt the two-component quantum-liquid state,[11–13] which combines superconductivity and superfluidity, being a new state of matter not yet observed in any other system.[14] However, to turn hydrogen into a metallic state pressures as high as 400–450 GPa are required,[13,15] which are hard to achieve at present. It was suggested that lower pressure may be sufficient if dissociation of the atoms is promoted by putting hydrogen into an environment with a different dielectric constant. That could be embodied by combining (diluting) hydrogen with some other element(s).[16,17] However, the question as to what extent metallic hydrogen features can be translated to such systems remains open. It has been suggested that high-temperature superconductivity as well as a melting of the hydrogen sublattice may occur at moderate pressures, for example, in hydrogen-dominant metallic alloys formed by the group IV elements, the tetrahydrides[18] (the systems with lower hydrogen content were studied in details over many years, but no the metallic hydrogen features were found[19]).

Silane SiH_4 and trivalent aluminum hydride AlH_3 have been studied recently both theoretically and experimentally. An insulator-to-metal transition and a transition to the superconducting state were reported to occur in SiH_4 at ~100 GPa,[20] which is in accord with the theoretical predictions.[21,22] However, subsequently, these results were questioned in light of the reactions of hydrogenation which was found to take place within the high-pressure chamber.[23] Also the data concerning structural and optical properties of the material obtained by different experimental groups are subject to discrepancies (see below).

Stoichiometric aluminum hydride forms at least six different metastable phases under ambient conditions.[24] The most stable and dense α phase is rhombohedral, space group $R\bar{3}c$, Al in $6b(000)$ and H/D in $18e(x,0,\frac{1}{4})$ with $x = 0.628$ in the hexagonal axes,[25] or alternatively Al in $2b(000)$ and H/D in $6e(x,\bar{x}+\frac{1}{2},\frac{1}{4})$ with $x = 0.878$ in the rhombohedral axes. The structure can also be viewed as a slightly distorted hcp hydrogen lattice with the parameters $a^* = a/\sqrt{3}$ and $c^* = c/3$ in which one-third of octahedral interstices are occupied by aluminum atoms (here a and c are the hexagonal parameters in $R\bar{3}c$).[26] The phase thereby represents dense packing of hydrogen atoms with a high degree of chemical precompression.[27]

Graetz *et al*. studied the α phase over an extended pressure region both experimentally by x-ray diffraction and theoretically by the density functional theory (DFT).[1] An indication of a monoclinic distortion of the structure was observed at pressures between 0 and 7 GPa (by broadening of the diffraction peaks). From the DFT calculations the monoclinic $C2/c$ polymorph was found to be stable with respect to decomposition to Al and H_2 and remains insulating up to at least 100 GPa. Subsequently, two structural phase transitions were predicted at elevated pressures by searching for a structure with minimum energy using the DFT simulations.[2,3] The first one should result in either an orthorhombic layered *Pnma* structure at $P \sim 34$ GPa (Ref. 2) or a hexagonal $P6_3/m$ structure at $P \sim 64$ GPa (Ref. 3). The high-pressure phases should be insulating. The second transition should take place either at 73 GPa (Ref. 2) or at 104 GPa (Ref. 3) and, according to both studies, should result in a high-symmetry cubic $Pm\bar{3}n$ phase which should be metallic. Goncharenko *et al*. experimentally observed two transitions by x-ray diffraction.[4] The first one occurred at pressures of 63 GPa and resulted in a low-symmetry phase whose structure was not solved. The second phase transition occurred at 100 GPa with formation of the $Pm\bar{3}n$ phase as predicted. From the electrical resistivity measurements the phase appeared metallic, but superconductivity was not observed down to 4 K.

Superconductivity in covalent-bonded systems is known to be a subject of delicate balance between many parameters, where strong electron-phonon coupling which enables the Cooper pairing may also result in instabilities leading to structure changes or to an insulating state.[28] A superconducting state with high critical temperature (if it is indeed characteristic of the hydrides) may appear over a narrow range of parameters (possibly for a very specific structure) and requires careful material design. In light of this a demand arises for understanding the driving forces of the structure changes and associated changes in electronic structure in the materials of interest.

Here we present a study where several new features in behavior of aluminum hydride were found by investigating evolution of the α phase under compression. The material was probed by means of Raman scattering, x-ray diffraction, and visual observation of optical transparency complemented by *ab initio* DFT-based simulations. In the optical experiments attention was paid to achieving equilibrium conditions as much as possible, first by allowing the sample to relax between pressure increases and second by making exposures to the probing irradiation (in case of Raman scattering) somewhat longer than it is actually needed for signal collection. A new light-induced phase transition was detected in AlD_3 by Raman scattering. Structure of the new phase was studied by the x-ray diffraction. The structure analysis points to the displacive type of the phase transition and also reveals a link between the low-pressure structure and the structure(s) appearing under compression. The equation of state (EOS) of the α phase for both isotopes AlD_3 and AlH_3 was measured by x-ray diffraction. The EOS data show no difference between the isotopes in terms of the thermodynamic behavior. A common phase diagram for both isotopes was constructed. The DFT calculations were applied to examine the band gap in the α phase. From the band gap behavior more insight into a mechanism of the light action was gained. The mechanism gives grounds to suggest that the kinetics is responsible for skipping the transition in AlH_3 (Ref. 4) and also confirms the displacive type of the structure transformation independently from the structure arguments. The sample transparency under increasing pressure supports the conclusion about the gap behavior derived from the DFT data and gives additional evidence for important role of the kinetics. Also, the transparency evolution data indicate a specific role of nonhydrostatic conditions, although this issue requires further study, which is beyond the scope of this paper.

II. EXPERIMENT

The samples were synthesized in the Kurnakov Institute of General and Inorganic Chemistry Russian Academy of Sciences from $LiAlH_4$($LiAlD_4$) and $AlCl_3$ by a technique similar to that described in Ref. 24. They had no less than 97% H/D relative to stoichiometric composition, and impurities of C, Li, Cl, and B were estimated to be about 0.6% in total. The synthesis was performed about 10 years before the experiments. Nevertheless, the deuteride look entirely white, though the hydride was slightly gray (for deuteride the sample was literally the same as that used by Goncharenko *et al*. in 1991[26]). Before the high-pressure experiments the samples were checked by x-ray diffraction, which showed no sings of contaminant phases.

High pressure was generated by a diamond-anvil cell (DAC) with the culets of 0.5 mm in diameter. The gasket was made of T301 stainless steel. It was preindented to 50 μm and then a hole with 100 μm in diameter was drilled. A platelet of the powder sample with $\sim$40 μm in size was placed into the hole rest of which was filled with helium serving as pressure transmitting medium (except for optical transmission observations, where no medium was used; see below). Pressure was measured by the ruby fluorescence method.

The Raman scattering measurements were made using the 0.6-m triple spectrometer coupled with nitrogen-cooled CCD multichannel detector. The sample was illuminated with the 514.5-nm line of an Ar^+ laser and the scattered light was analyzed at 135° with respect to the incoming beam. The x-ray diffraction experiments were performed at beamline ID9 of the European Synchrotron Radiation Facility (ESRF). For the EOS measurements of the α phase the beamline was operating in the white-beam energy-dispersive mode. For the structure determination of the new high-pressure phase it was operated in the monochromatic-beam angular-dispersive mode and the powder diffraction patterns were recorded by the image plate area detector. The geometry of the experiment was similar to that described in Ref. 29. In both modes a typical exposure time was $\sim$30 min. All measurements were made at room temperature.

The density functional calculations were performed within the generalized gradient approximation (GGA) as implemented by the QUANTUM ESPRESSO *ab initio* simulation package.[30] The PBE functional[31] was applied with the ultrasoft pseudopotentials (generated by the CAMPOS code) used to describe the core electrons. The k-point grid for the Brillouin-zone sampling was generated by the Monkhort-Pack method. The plane-wave basis cutoff energy was 36 Ry.

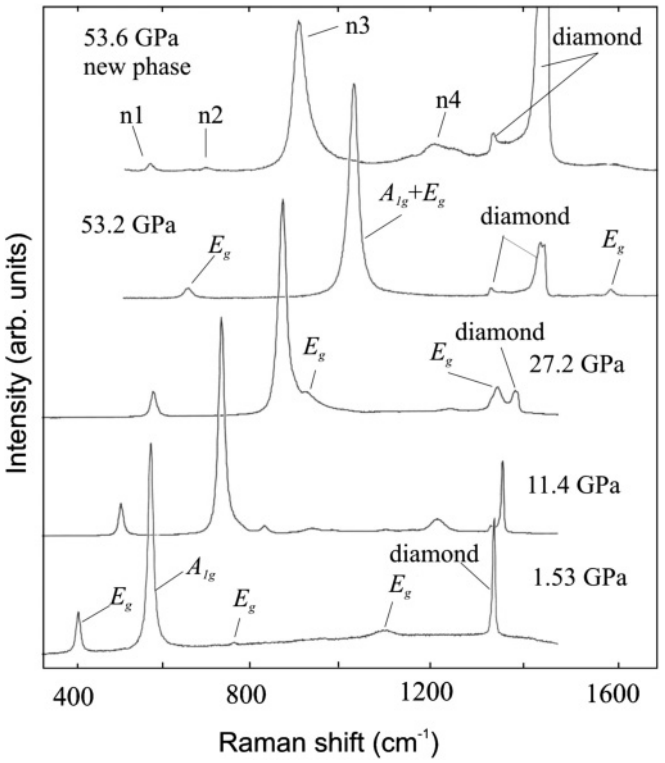

FIG. 1. Raman spectra of AlD_3 at different pressures (pressure is increased). n1, n2, n3, and n4 denote the peaks in the light-induced phase; other annotations are described in Ref. 32. The difference in pressure between the upper two patterns (53.2 and 53.6 GPa) resulted from spontaneous drift during the phase transformation.

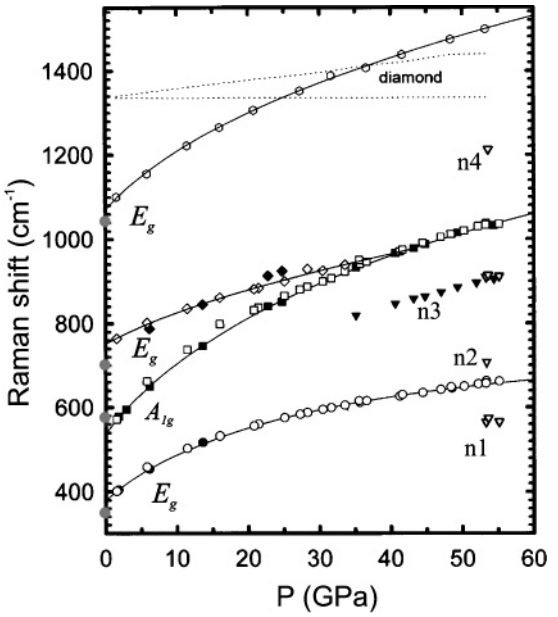

FIG. 2. Frequency of the Raman modes for AlD_3 as a function of pressure. Open symbols correspond to compression; solid symbols correspond to decompression. Inverted triangles are related to the new phase; gray circles on the verticle axis, theoretical values from Ref. 33; solid lines, guides for the eye; dotted lines, the region near 1350 cm^{-1} with high background resulting from the Raman peak from diamond. Annotations are the same as in the previous figure.

III. RESULTS

Figure 1 shows evolution of the Raman spectra for AlD_3 with pressure. Under ambient conditions laser irradiation causes quick decomposition of the compound even at minimal laser power. However, under compression the material is stabilized, so the data were acquired at pressures above ~1 GPa. All four modes predicted by the factor-group analysis[32] are observable at low pressures. They were identified by comparison of the peak frequencies with the calculated values for AlH_3 (Ref. 33) reduced by $\sqrt{2}$ (Fig. 2). All the modes exhibit positive pressure shifts in frequency although with different rates, in accord with the results obtained for AlH_3 (Ref. 34). At pressure $P \sim 35$ GPa frequencies of the A_{1g} and of the E_g modes become equal, so that at higher pressures only three modes are observed. At $P \sim 53$ GPa sufficiently long (~20 min) exposure to the laser irradiation used to excite the Raman signal results in the disappearance of the initial peaks in the spectrum and in the appearance of three new distinct peaks as well as a broad feature with a maximum at 1200 cm^{-1}, all having much lower intensities (see upper spectrum in Fig. 1). These changes were attributed to a phase transition. The onset of the transition is accompanied by change of sample color under the laser spot, so it is easy to distinguish between parts belonging to the different phases [Fig. 3(a)]. Coexistence of both phases was observed during at least several days. The transition thereby appears stimulated by light (green in our case) provided that pressure as high as 53 GPa is reached. Under decreasing pressure the strongest peak of the new phase persisted down to ~35 GPa. At yet lower pressures three peaks corresponding to the low-frequency modes of the initial α phase were observed, although their intensities were weak.

To examine possible structure changes at the phase transition x-ray diffraction measurements were performed. Before the measurements the sample was compressed to 53 GPa and exposed to the laser irradiation by scanning with the focused spot until the color of the whole sample changed and the Raman spectra showed no presence of the low-pressure phase. The x-ray diffraction pattern appeared drastically different from that of the α phase (Fig. 4). Since the Raman scattering data indicate the presence of a pressure loop, several exposures were taken under decreasing pressure down to 34 GPa. It was found that most of the peaks including all the strong ones did not change with pressure (except for a shift in the angular positions), whereas some weak peaks, such as three peaks at $2\theta < 9.5°$ and four at $11° < 2\theta < 13.5°$, diminished and vanished completely at 34 GPa. When pressure was raised again to 47 GPa they reproducibly reappeared.

Structure analysis was performed using the FULLPROF software package.[35] Because of the large difference in the scattering amplitudes for hydrogen and aluminum atoms the x-ray diffraction measurements provide data only on the aluminum sublattice. The structure reconstructed from the stable peaks (only those are seen at 34 GPa; Fig. 4) was found to be monoclinic described by the space group $P2_1/c$ with the atoms located in general positions $4e(xyz)$ (see Table I). The monoclinic unit cell (**abc**) and the rhombohedral one (**ABC**) are connected by the orientation relationships as follows: $\mathbf{a} = -\mathbf{A} - \mathbf{C}, \mathbf{b} = -\mathbf{A} + \mathbf{C}$ and $\mathbf{c} = \mathbf{A} + \mathbf{B} + \mathbf{C}$ with the origin shifted by $-\frac{1}{2}\mathbf{A}$ (Fig. 5, top). So the structure of the

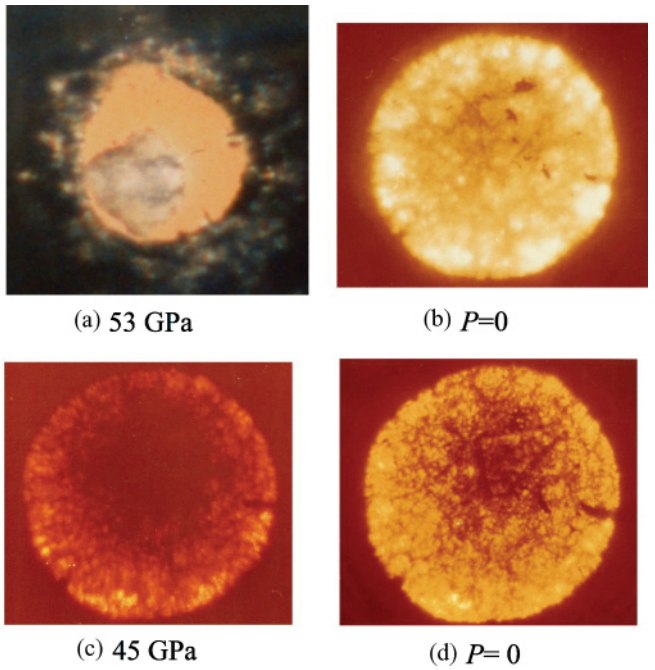

FIG. 3. (Color online) Images of the sample. (a) A two-phase sample under combined transmission and epi-illumination. Horizontal laser trace (new phase) is seen in the middle of the droplet. The parts of the α phase have lighter color, which are above and below the new-phase strip. The rest of the hole is filled with He. The ruby ball is seen at the right edge. (b)–(d) The sample is under transmission illumination (a high-pressure Xe lamp was used as the light source). No medium was used. Photo (b) was taken before pressure loading, photo (d) after unloading (here the ruby chip is clearly seen).

new phase can be obtained from the α phase by shifts of the neighboring $(101)_{(\mathbf{ABC})}$ planes oppositely to each other in the directions $[\bar{1}01]_{(\mathbf{ABC})}$ and $[10\bar{1}]_{(\mathbf{ABC})}$, followed by distortion of the lattice (compare Fig. 5, center and bottom). The displacive mechanism of the transformation is confirmed by behavior of the peaks under decreasing pressure. First, at 34 GPa the peaks are almost two times broader than at 53 GPa (Fig. 4). The broadening indicates increase of lattice strains which usually precede lattice shifts. Second, the static Debye-Waller factor (given by the parameters β_{ij} in FULLPROF) appears notably nonisotropic, indicating that random displacements of the atoms in the direction $[010]_{(\mathbf{abc})}$ are nearly order of

TABLE I. Parameters of the aluminum sublattice in the light-induced high-pressure phase AlD_3. Space group $P2_1/c$ (No. 14), Al in $4e(xyz)$, $Z = 4$ (for comparison, parameters for the α phase at 53 GPa are given in square brackets).

P(GPa)	53.2		34.27
a (Å)	6.292(1)	[7.272]	6.565(2)
b (Å)	4.074(1)	[3.657]	4.170(1)
c (Å)	8.789(1)	[10.438]	9.170(2)
β°	160.46(1)	[163.12]	160.67(1)
V(Å^3)	75.36(4)	[80.60]	83.09(6)
x	0.288(2)	[$\frac{1}{4}$]	$\frac{1}{4}$
y	0.358(2)	[$\frac{1}{4}$]	0.355(2)
z	0.020(1)	[0]	0

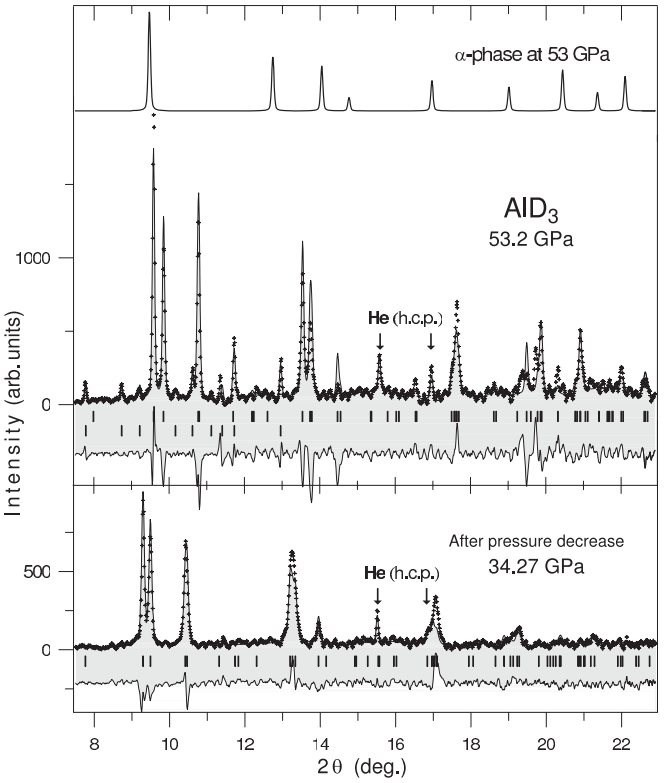

FIG. 4. X-ray diffraction patterns for the light induced high-pressure phase AlD_3, $\lambda = 0.447$ Å. Top pattern is for $P = 53.2$ GPa; the bottom one is for $P = 34.27$ GPa. The reference pattern for the α phase at $P = 53$ GPa is given on top. +, experimental points; solid lines, calculated profiles for the structure parameters from Table I ($R_F = 16.5\%$ for 53.2 GPa, $R_F = 14.1\%$ for 34.27 GPa); below are the difference curves. Vertical dashes mark positions of the Bragg peaks and of superstructure ones for 53.2 GPa (lower series). Arrows point to the peaks from the helium medium.

magnitude greater than in other directions. In other words, the maximum strain appears along the $[010]_{(\mathbf{abc})} = [\bar{1}01]_{(\mathbf{ABC})}$, which is exactly in the direction of future shifts which should restore the α phase. The weak peaks which are developed with pressure and are not indexed in the (**abc**) unit cell (see top pattern in Fig. 4) indicate development of a superstructure formed by regular displacements of the Al atoms with the period covering more than one unit cell. Because of low signal to noise, full structure determination is not simple. Nevertheless, using the matching mode in FULLPROF the superstructure peaks were indexed in the enlarged cell (3**a**, 3**b**, 3**c**), the space group remained the same, $P2_1/c$. Accordingly, the propagation vector of the superlattice is $\mathbf{k}_2 = (\frac{1}{3}\frac{1}{3}\frac{1}{3})_{(\mathbf{a^*b^*c^*})}$ [here ($\mathbf{a^*b^*c^*}$) is the reciprocal cell for the monoclinic unit cell]. From the anisotropic displacement parameters for the structure with the (**abc**) cell one can suggest that in the superstructure the atoms are mainly displaced in the plane (**ac**). Interestingly, the space group $P2_1/c$ is a subgroup of $C2/c$, which in turn is a subgroup of $R\bar{3}c$ (Ref. 36). This means that the $P2_1/c$ phase is a superstructure over the $R\bar{3}c$ α phase with the propagation vector $\mathbf{k}_1 = (\frac{1}{2}0\frac{1}{2})_{\mathbf{A^*B^*C^*}}$ [here ($\mathbf{A^*B^*C^*}$) is the reciprocal cell for the rhombohedral unit cell]. Thus, the complicated low-symmetry structure of the new phase appears genetically linked with the original

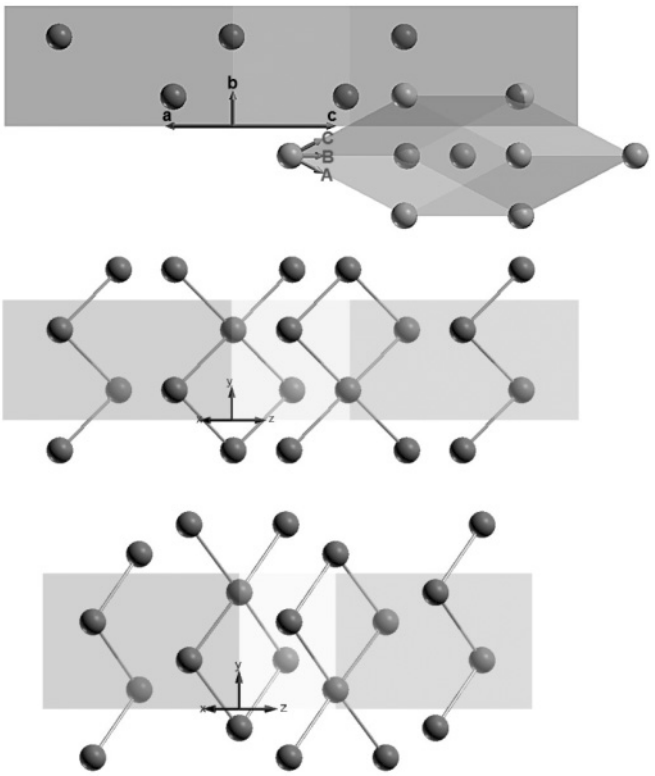

FIG. 5. The laser-induced structure change. (Top) The relationship between the rhombohedral and the monoclinic unit cells for the α phase. (Center) Al sublattice of the α phase at 53 GPa (monoclinic system). (Bottom) Al sublattice of the light-induced phase at 53 GPa.

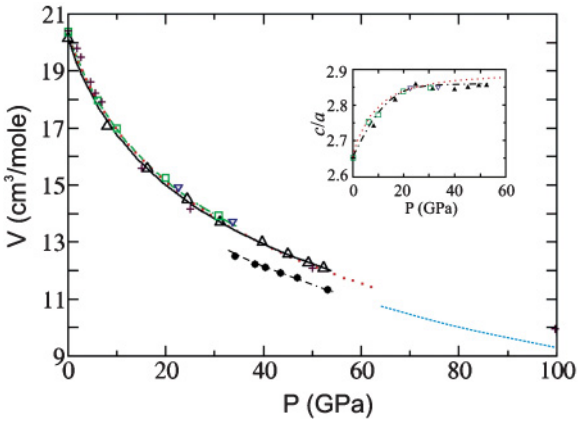

FIG. 6. (Color online) Equation of state (main figure) and pressure dependence of the c/a ratio (inset) of the α phase. The cell parameters at the ambient pressure are (in hexagonal axes): $a = 4.452$ Å, $c = 11.819$ Å for AlH_3; $a = 4.434$ Å, $c = 11.790$ Å for AlD_3. Triangles, AlD_3 (He medium); squares, AlH_3 in He medium; inverted triangles, AlH_3 in H_2 medium; solid circles, light-induced phase for AlD_3; crosses, AlH_3 from Ref. 1; solid and long-dashed lines, Vinet *et al*. function fits for AlD_3 and AlH_3, respectively; dotted line, α-AlH_3 from Ref. 4; short-dashed line, phase II for AlH_3 from Ref. 4; dash-dotted lines, guides for the eye. For H/D the sublattice of the α phase the ratio c^*/a^* (see main text) is increased from 1.53 at $P = 0$ to 1.645 at $P > 30$ GPa.

one. Namely, it results from the formation of two sequential superstructures.

The EOS of the α phase has been measured for both isotopes. AlD_3 and AlH_3 were compressed up to 52 and 32 GPa, respectively. The hydride was probed using both He and H_2 pressure mediums in order to check possible effect of the medium. From 5 to 10 diffraction peaks for different pressures were clearly observable with full width at half maximum (FWHM) between 0.4 and 0.65 keV. All the reflections were indexed in the rhombohedral unit cell and the unit cell parameters were derived by least-squares fitting to the positions of the reflections. No effect is observed between the H_2 and He mediums. The pressure-volume data for each isotope were fitted by the Vinet *et al*. function,[37] where K_0 and K' were varied and V_0 was fixed to the ambient pressure values. Both AlD_3 and AlH_3 was found to be represented by the same function with $K_0 = 37.4(6)$ GPa and $K' = 4.20(16)$.

The EOS from our data essentially coincides with that recently determined by Goncharenko *et al*.[4] and also is in reasonable agreement with combined experimental and theoretical EOS by Graetz *et al*.[1] (Fig. 6). Earlier data from Refs. 38 and 26 (not shown here), as well as the experimental points from Ref. 1, tend to lie above our curve. This difference is attributed to nonhydrostatic conditions in these previous experiments (silicon and paraffin oil were used as pressure-transmitting medium in Ref. 38 fluorinert was used in Ref. 1 and no medium was used in Ref. 26).

The behavior of the band gap was examined, first, by visual observation of optical transmission[39] and, second, by the DFT-based electronic structure calculations. The optical observations were made using a compact sample prepared by tight filling of the gasket hole with the powder material with no pressure-transmitting medium (if He or H_2 is present in the gasket hole, the sample appears porous, which prevents unambiguous identification of its color). Several runs were made with both isotopes AlH_3 and AlD_3. We found blackness appearing by nucleation normally first in the vicinity of the ruby chip, followed by propagation outward and increasing density at the chip as pressure is increased. The process occurs gradually so no definite specific pressure value can be assigned to the point when it starts, but definitely the sample becomes opaque at pressures about 45–48 GPa [Fig. 3(c)]. During one of the runs at about 22 GPa pressure the sample was left overnight. The next day distinct blackness appeared around the ruby chip with no change in the pressure. Under further compression the sample became black, similar to that shown in the photo. When pressure is released to zero the opaqueness did not disappear completely [Fig. 3(d)]. No noticeable difference between the isotopes was observed.

The pressure dependence of the band gap ΔE as it appears from the electronic structure calculations is depicted of Fig. 7. The plot was obtained in the following way. First, for a given sample density the structure was optimized with respect to H atoms positions by minimizing the lattice energy where H atoms were allowed to relax while the shape of the rhombohedral unit cell (see the inset in Fig. 6) was fixed by the positions of the Al atoms known from the experiment (the k-point grid dimensions were $10 \times 10 \times 6$). Then for the optimized structure electronic density of states was calculated

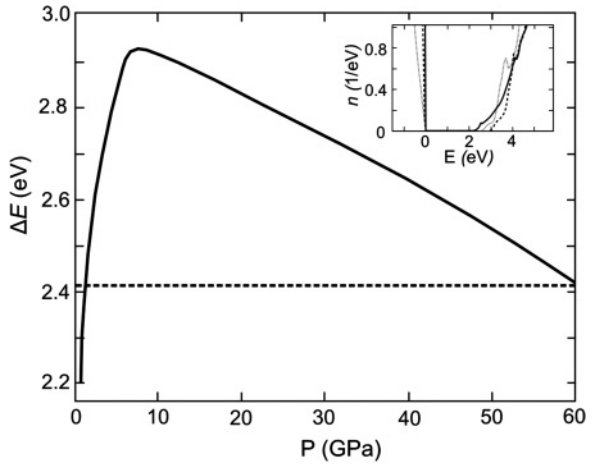

FIG. 7. Evolution of the band gap with pressure. The dashed line indicates the photon energy of the laser used $E_{\text{photon}} = 2.41$ eV. In the inset, examples of the electronic density of states vs electron energy in the vicinity of band gap for $P = 0$ (solid line), $P = 8$ GPa (dashed line), and $P = 50$ GPa (dotted line).

(using the $10 \times 10 \times 10$ k-point grid size), giving the band gap (examples are shown in the inset in Fig. 7). This procedure was performed for several density points within pressure interval from 0 to ~60 GPa and conversion to the pressure scale was made using the experimental EOS. The band gap was studied by several groups using various DFT flavors.[1–3,40] At zero pressure the values obtained range from 1.99 eV (Ref. 3) to 3.54 eV (Ref. 40). It is well known that generally used density functionals like the PBE-GGA used here tend to underestimate the band gaps. So the greater values look more plausible. Nevertheless, we note that our data $\Delta E = 2.2$ eV agree with the results obtained by Graetz *et al.*[1] Also our results are in qualitative agreement with this work in the sense that evolution of the gap under increasing density in both calculations is nonmonotonic, first increasing then decreasing. However, whereas in Ref. 1 the maximum is reached at about 50 GPa, in our calculations a remarkably sharp increase of the gap is observed at low pressures, giving a maximum around 8 GPa. Our curve crosses the photon energy of the green laser ($E_{ph} = 2.41$ eV) just within a few gigapascals that is in accord with the experimental observations when the material is decomposed under the laser light at ambient pressure while being stabilized under compression. This fact gives us additional confidence in correctness of the numerical results obtained, although the conclusions made below are based solely on the fact that the band gap value at high pressures remains greater than the photon energy.

IV. DISCUSSION

It appears from the existing experimental data (both the present study and by Goncharenko *et al.*[4]) that the α phase transforms to different phases for AlD_3 and for AlH_3. Also in the deuteride the transition occurs at a pressure 10 GPa lower than in the hydride. These facts cannot be explained simply by difference in the vibrational energy since the EOS does not exhibit a significant isotope effect. Instead, this appears to be dependent on experimental conditions. In our case the

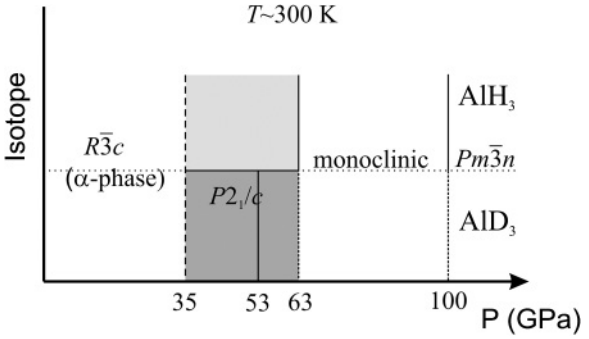

FIG. 8. Generalized phase diagram of aluminum hydride at room temperature. Solid vertical lines depict experimentally observed phase boundaries. The long-dashed line indicates a proposed lower boundary for the $P2_1/c$ phase. The short-dashed lines indicate expected phase boundaries for AlD_3 at higher pressures.

transition in AlD_3 is stimulated by visible light. Currently, many materials (ranging from the spin-crossover and the charge-transfer systems[41] to biological objects[42]) are known where light induces smaller or greater structural changes. Mechanisms of the light action generally are complex even in "simple" systems—α-Si:H, for example[43]—and still not completely clear. Generally, two basic processes are involved: the electron excitation (leading, for example, to the metastable phases[44]) and electron-phonon coupling.[41,45] As mentioned above, in AlH_3 the band gap given by the DFT calculations at all pressures except narrow region near zero remains greater than the photon energy of the laser irradiation used (Fig. 7). This means that at 53 GPa the photon energy is not sufficient to excite the electrons across the band gap. So, the mechanisms implying bond weakening/breaking appear not to be the case. We adopt then that a phonon-driven displacive structural transformation[46] takes place (as described above by structural arguments), which occurs due to (sufficiently) strong electron-phonon coupling in the α phase.[45] Thus, in our experiment light irradiation promoted structure changes which in all probability were hindered by slow kinetics. The transition then occurred at lower pressure and resulted in a phase which did not manifest itself previously in AlH_3 (Ref. 4). The laser light thereby fulfills a kind of "optical annealing," the phenomenon also known in other systems where structural changes are stimulated by light (see, for example, Ref. 47). Essentially, this is the same process as "usual" thermal annealing since in both cases annealing is driven by phonons. However, while the population of thermally exited phonons obeys the Boltzmann distribution, light may excite some specific phonons depending on what channel of energy transfer from the electromagnetic wave to the crystal lattice is in action. Which particular phonons are responsible for the annealing (and whether or not they are involved in the Cooper pairing, if any) is an intriguing question requiring further studies.

Our data confirm the theoretical predictions[2,3] in the sense that at pressures of several tens of gigapascals the α phase becomes energetically unfavorable with respect to a number of other phases with different structures. However, the experimentally observed structural behavior above the transition point turned out to be unexpectedly complex, which was

not anticipated theoretically. This reflects existing difficulties in prediction of new phases in hydrogen-rich compounds since several structures may have close energies. The link empirically found between the structures via group-subgroup relationships as above may offer a way to predict phase sequences under densification alternative to probing different structures with respect to minimal energy. At this stage the region of applicability of such an approach requires more verification.[48]

In Fig. 8 a proposed phase diagram for aluminum hydride constructed using the cumulative data for both isotopes is shown. Under compression at room temperature the α phase is transformed to the $P2_1/c$ one by the first-order phase transition with ~6% volume jump (since positions of the H atoms remain unknown, symmetry of the whole structure may actually be lower). The $P2_1/c$ phase is characterized by development of the superstructure with no symmetry change in the Al sublattice. Although the phase transition occurs at 53 GPa, we believe that more physically meaningful phase boundary is around 35 GPa, where the $P2_1/c$ lattice is not distorted. The lattice distortion when it becomes sufficiently large should result in another structural phase transition, which was actually observed at 63 GPa in Ref. 4. Whether there is a group-subgroup relationship between the structures of these phases requires further study (including structure solution of the phase between 63 and 100 GPa). At this stage one may only state that the transition seems to be of the second order since no volume jump is expected from the EOS (Fig. 6). At about 100 GPa the transition to the metallic phase with cubic symmetry occurs as reported in Ref. 4.

In our observations the sample becomes black at pressure about 45–48 GPa, which is drastically different from the previous study,[4] where blackening was observed at $P \sim$ 100 GPa (prior to the transition to the cubic metallic phase). The way the opacity appears in our study (nucleation under nonhydrostatic conditions) suggests the formation of a new phase rather than gradual gap reduction (in the latter case one should observe the sequential color change). This is also consistent with the temporal lag at $P \sim 22$ GPa mentioned above, which therefore can be attributed to the slow rate of the opaque phase formation. The nature of this phase in not obvious. The local anisotropic stress may be much higher than average pressure indicated by the ruby gauge. Yet a transition to this phase may be driving by a shear component. So, whether the opaque phase is the $P2_1/c$ one or either of the phases observed in Ref. 4 or some yet-unknown phase requires further study.

Interestingly, the overall situation resembles that existing in the case of SiH_4. Indeed, three pressure ranges were reported where silane becomes black: The first one is near 100 GPa,[49] the second ranges from 50 to 65 GPa to 76 GPa (Ref. 20), and the third one is at 27–30 GPa.[50] The origin of these discrepancies remains uncertain. An amorphous state was recently found at pressure between 60 and 90 GPa (Ref. 51), which previously was missed. Slow rate of the structural transformations (up to several months) is reported in both studies (Refs. 20 and 51) and a major role of kinetics was pointed out to explain sequence of phases appearing under compression.[20] Whether slow kinetics is an inherent property of hydrogen-rich compounds is not clear. Nevertheless, it seems to play a key role in the sense that it significantly affects the phenomena observed in the experiments.

In conclusion, the behavior of aluminum hydride under pressure appears more diverse than it was predicted theoretically and previously found experimentally. The material turned out to be sensitive to visible light. When the α phase becomes energetically unfavorable under compression, green laser light stimulates a structural transition to a phase, which was not observed previously in this pressure region. The structure change is of displacive type and appears to occur due to strong electron-phonon coupling in the α phase. The resulting low-symmetry structure is a superstructure based on the α phase and it tends to further superstructure formation as pressure is increased. There is discrepancy between existing experimental data concerning the pressures at which the sample becomes black. At least partially this can be attributed to nonhydrostatic conditions. Also kinetics should be accounted for as a key factor when interpreting the experimental data.

ACKNOWLEDGMENTS

The authors thank M. Hanfland for his generous help with the X-ray measurements, S. Bakum for supplying us with the sample, and M. Andreichikov for performing the DFT calculations. We thank B. Ostrovskii and V. Somenkov for reading the manuscript and making valuable comments. Experiments performed at University of Oxford before 1998. SPB and APJ acknowledge the Royal Society as well as UK Natural Environment Research Council for support from Grants GR9/10912 and GR9/01570. SPB acknowledges V. Kvardakov for support at Kurchatov Institute. Paper preparation was supported by Federal Agency for Science and Innovation (Russian Federation) under contracts No 1.164.1 2.HB12 and No 02.518.11.7144.

*s.besedin@mpic.de; present address: Max Plank Institute für Chemie, J-J-Becherweg 27, D-55128 Mainz, Germany.

[1] J. Graetz, S. Chaudhuri, Y. Lee, T. Vogt, J. T. Muckerman, and J. J. Reilly, Phys. Rev. B **74**, 214114 (2006).

[2] C. J. Pickard and R. J. Needs, Phys. Rev. B **76**, 144114 (2007).

[3] P. Vajeeston, P. Ravindran, and H. Fjellvåg, Chem. Matter. **20**, 5997 (2008).

[4] I. Goncharenko, M. I. Eremets, M. Hanfland, J. S. Tse, M. Amboage, Y. Tao, and I. A. Trojan, Phys. Rev. Lett. **100**, 045504 (2008).

[5] J. Graetz and J. J. Reilly, J. Alloys Compd. **424**, 262 (2006).

[6] R. Zidan, B. L. Garcia-Diaz, C. S. Fewox, A. C. Stowe, J. R. Gray, and A. G. Harter, Chem. Commun. **25**, 3717 (2009).

[7] L. Schlapbach and A. Züttel, Nature (London) **414**, 353 (2001).

[8] J. Nagamatsu, N. Nakagawa, T. Muranaka, Y. Zenitani, and J. Akimitsu, Nature (London) **410**, 63 (2001).
[9] N. W. Ashcroft, Phys. Rev. Lett. **21**, 1748 (1968).
[10] C. F. Richardson and N. W. Ashcroft, Phys. Rev. Lett. **78**, 118 (1997).
[11] E. G. Brovman, Yu. Kagan, and A. Kholas, Sov. Phys. JETP **35**, 783 (1972).
[12] N. W. Ashcroft, J. Phys. Condens. Matter **12**, A129 (2000).
[13] S. A. Bonev, E. Schwegler, T. Ogitsu, and G. Galli, Nature (London) **431**, 669 (2004).
[14] E. Babaev, A. Sudbø, and N. W. Ashcroft, Nature (London) **431**, 666 (2004).
[15] P. Loubeyre, F. Occelli, and R. LeToullec, Nature (London) **416**, 613 (2002).
[16] R. J. Gillman, Phys. Rev. Lett. **26**, 546 (1971).
[17] A. E. Carlsson and N. W. Ashcroft, Phys. Rev. Lett. **50**, 1305 (1983).
[18] N. W. Ashcroft, Phys. Rev. Lett. **92**, 187002-1 (2004).
[19] In the hydrides of the transitional metals, which are metallic already at atmospheric pressure, hydrogen exhibits high mobility and the lattice-gas behavior [V. A. Somenkov and S. Sh. Shil'stein, Z. Phys. Chem. N.F. **117**, 125 (1979)]. But this seems to have little in common with the metallic hydrogen liquid state because behavior of the hydrides is underlined by narrow *d* bands of the host metals [E. G. Maksimov and O. A. Pankratov, Sov. Uspehi Fis. Nauk **18**, 481 (1976); Y. Fukai, *The Metal-Hydrogen System* (Springer-Verlag, Berlin, New York, 1993)]. Metallization was reported to occur in hydrogen sulfide H_2S at pressure of 96 GPa, but again this happens due to formation of S=S bonds with hydrogen playing a minor role [M. Sakashita, H. Yamawaki, H. Fujihisa, K. Aoki, S. Sasaki, and H. Shimizu, Phys. Rev. Lett. **79**, 1082 (1997)].
[20] M. I. Eremets, I. A. Trojan, S. A. Medvedev, J. S. Tse, and Y. Yao, Science **319**, 1506 (2008).
[21] J. Feng, W. Grochala, T. Jaron, R. Hoffmann, A. Bergara, and N. W. Ashcroft, Phys. Rev. Lett. **96**, 017006 (2006).
[22] C. J. Pickard and R. J. Needs, Phys. Rev. Lett. **97**, 045504 (2006).
[23] O. Degtyareva, J. E. Proctor, C. L. Guillaume, E. Gregoryanz, and M. Hanfland, Solid State Commun. **149**, 1583 (2009).
[24] F. M. Brower, N. E. Matzek, P. F. Reigler, H. W. Rinn, C. B. Roberts, D. L. Schmidt, J. A. Snover, and K. Terada, J. Am. Chem. Soc. **98**, 2450 (1976).
[25] J. W. Turley and H. W. Rinn, Inorg. Chem. **8**, 18 (1969).
[26] I. N. Goncharenko, V. P. Glazkov, A. V. Irodova, and V. A. Somenkov, Physica B **174**, 117 (1991).
[27] We use r_s as a measure of average valence electron density, which is defined in the usual way as $4/3\pi r_s^3 a_0^3 = V/N_e$, where $a_0 = 0.529$ Å (the Bohr radius) and N_e is number of valence electrons in volume V. For AlH_3 at 1 atm $r_s = 2.07$ (that is higher than, for example, for GeH_4, as well as for the trihydrides of the rare-earth metals).
[28] J. E. Moussa and M. L. Cohen, Phys. Rev. B **74**, 094520 (2006).
[29] S. P. Besedin, A. P. Jephcoat, M. Hanfland, and D. Häusermann, Appl. Phys. Lett. **71**, 470 (1997).
[30] P. Giannozzi, S. Baroni, N. Bonini, M. Calandra, R. Car, C. Cavazzoni, D. Ceresoli, G. L. Chiarotti, M. Cococcioni, I. Dabo, A. D. Corso, S. de Gironcoli, S. Fabris, G. Fratesi, R. Gebauer, U. Gerstmann, C. Gougoussis, A. Kokalj, M. Lazzeri, Layla Martin-Samos, Nicola Marzari, Francesco Mauri, Riccardo Mazzarello, S. Paolini, A. Pasquarello, L. Paulatto, C. Sbraccia, S. Scandolo, G. Sclauzero, A. P. Seitsonen, A. Smogunov, P. Umari, and R. M. Wentzcovitch, J. Phys. Condens. Matter **21**, 395502 (2009).
[31] J. P. Perdew, K. Burke, and M. Ernzerhof, Phys. Rev. Lett. **77**, 3865 (1996).
[32] The unit cell of the α phase contains two Al and six H/D atoms. Symmetries of the occupied sites are S_6 and C_6, respectively. Twenty-four normal modes with wave vector $k \approx 0$ belong to the irreducible representation $\Gamma_{\rm crys} = A_{1g} + 2A_{2g} + 3E_g + 2A_{1u} + 3A_{2u} + 5E_u$ of the factor group D_{3d}. Four modes—the fully symmetric A_{1g} and three doubly degenerate E_g—are Raman active. They are associated with vibration of the H/D sublattice. Also, there are two acoustic modes—the longitudinal A_{2u} and the doubly degenerate transverse E_u—as well as six infrared active modes $2A_{2u} + 4E_u$. The remaining optical modes are silent.
[33] C. Wolverton, V. Ozolins, and M. Asta, Phys. Rev. B **69**, 144109 (2004).
[34] M. Tkacz, T. Palasyuk, J. Graetz, and S. Saxena, J. Raman Spectrosc. **39**, 922 (2008).
[35] T. Roisnel and J. Rodriguez-Carvajal, Mater. Sci. Forum **378–381**, 118 (2001).
[36] *International Tables for Crystallography*. Volume A1: Symmetry Relations between Space Groups, edited by H. Wondratschek and U. Müller (Kluwer Academic Publishers, Dordrech, Boston, London, 2004).
[37] Pressure as a function of volume at a given temperature T is written as $P_T = 3K_0(\frac{V}{V_0})^{-2/3}[1-(\frac{V}{V_0})^{1/3}]\exp\{\frac{3}{2}(K_0'-1)[1-(\frac{V}{V_0})^{1/3}]\}$, where K_0 is a bulk modulus, $K_0' = \partial K_0/\partial P$ [P. Vinet *et al.*, J. Phys. C **19**, L467 (1987)].
[38] B. Baranowski, H. D. Hochheimer, K. Strössner, and W. Hönle, J. Less-Common Met. **113**, 341 (1985).
[39] Here we describe early observations by V. N. Kachinskii, S. P. Besedin, I. N. Makarenko, S. M. Stishov, V. P. Glazkov, and S. Sh. Shil'stein made in 1985 using fresh from production samples (unpublished). The results were essentially reproduced in the course of the Raman and x-ray measurements using samples from the same source [A. P. Jephcoat and S. P. Besedin, *ESRF Report*, exp. HS104, 1995].
[40] M. J. van Setten, V. A. Popa, G. A. de Wijs, and G. Brocks, Phys. Rev. B **75**, 035204 (2007).
[41] A. Radosz, K. Ostaziewicz, P. Magnuszewski, L. Radosiński, F. V. Fusmartsev, and J. H. Sampson, Phys. Status Solidi B **242**, 454 (2005).
[42] A. B. Wöhri, G. Katona, L. C. Johansson, E. Fritz, E. Malmerberg, M. Andersson, J. Vincent, M. Eklund, M. Cammarata, M. Wulff, J. Davidsson, G. Groenhof, and R. Neutze, Science **328**, 630 (2010).
[43] T. A. Abtew and D. A. Drabold, J. Optoelectron. Adv. Mater. **8**, 1979 (2006).
[44] K. Nasu, *Photoinduced Phase Transitions* (World Scientific Publishing, Singapore, 2004).
[45] R. Atta-Fynn, P. Biswas, and D. A. Drabold, Phys. Rev. B **69**, 245204 (2004).
[46] A. D. Bruce and R. A. Cowley, *Structural Phase Transitions* (Taylor & Francis, London, 1981).
[47] X. Zhang and D. A. Drabold, Phys. Rev. Lett. **83**, 5042 (1999).
[48] The first-order phase transitions with the group-subgroup relationships is known to be characteristic of many hydrides of transitional metals [T. Schober and H. Wenzl, in *Hydrogen in Metals II, Application-Oriented Properties*, edited by G. Alefeld and J. Volkl (Springer-Verlag, Berlin, Heidelberg, New York, 1978); V. A.

Somenkov and S. S. Shil'shtein, Prog. Mater. Sci. **24**, 267 (1980)]. However, in the case of aluminum hydride one finds such a transition in a stoichiometric hydride.

[49]L. Sun, A. L. Ruoff, Ch-Sh. Zha, and G. Stupian, J. Phys. Condens. Matter **18**, 8573 (2006).

[50]X-J. Chen, V. V. Struzhkin, Y. Song, A. F. Goncharov, M. Ahart, Zh. Liu, H. K. Mao, and R. J. Hemley, Proc. Natl. Acad. Sci. USA **105**, 20 (2008).

[51]M. Hanfland, J. E. Proctor, C. L. Guillaume, O. Degtyareva, and E. Gregoryanz, Phys. Rev. Lett. **106**, 095503 (2011).